PHOTOINJECTOR PRODUCTION OF A FLAT ELECTRON BEAM

E. Thrane, University of Michigan, C. Bohn (presenter) Northern Illinois University and FNAL*,
N. Barov, D. Mihalcea, Northern Illinois University, Y. Sun, University of Chicago,
K. Bishofberger, D. Edwards, H. Edwards, S. Nagaitsev, J. Santucci, FNAL,
J. Corlett, S. Lidia, Lawrence Berkely National Laboratory, S. Wang, Indiana University,
R. Brinkmann, J.-P. Carneiro, K. Desler, K. Flöttmann, DESY Hamburg
I. Bohnet, DESY Zeuthen, M. Ferrario, INFN-Frascati

Abstract

At LINAC2000 [1] and PAC2001 [2] we reported our verification of the round beam (comparable transverse emittances) to flat beam (high transverse emittance ratio) transformation described by Brinkmann, Derbenev, and Flöttmann [3]. Here, we report progress in improvement between experiment and predictions of simulation.

1 INTRODUCTION

Four years ago, Ya. Derbenev invented an optics maneuver for transforming a beam with a high ratio of horizontal to vertical emittance—a "flat beam" as typically produced through radiation damping in an electron storage ring—to one with equal emittances in the transverse degrees-of-freedom—a "round beam"[4]. High energy electron cooling at the TeV energy scale was the motivation.

Three years ago, R. Brinkmann and K. Flöttmann of DESY joined with Derbenev in a paper that reverses the process—obtain a flat beam from a round beam produced from the cathode of an electron gun[3]. Their idea was the simplification or even elimination of the electron damping ring in a linear collider project.

The principle may be characterized as follows. If the cathode of an electron gun is immersed in a solenoidal magnetic field, the beam at production acquires a canonical angular momentum directed along the beam axis. Upon exit from this field, the beam then has a kinematic angular momentum directed in the same sense. Subsequent passage through a quadrupole channel having a 90 degree difference in phase advance between the two transverse degrees of freedom can result in a flat beam through appropriate choice of parameters. A simple-minded version of the basic principle may be found in our paper at LINAC2000[1]. A thorough treatment has been developed by Burov, Derbenev, and Nagaitsev[5].

The intent of the present experiment was to demonstrate the round-to-flat transformation, compare the results with simulation, and verify that the demonstration was not obscured by other processes. Earlier reports on this work have appeared in the proceedings of LINAC2000[1] and PAC2001[2].

*The Fermi National Accelerator Laboratory is operated under contract with the US Department of Energy

2 ANGULAR MOMENTUM AND THE CORRELATION MATRIX

The solenoidal magnetostatic field may be described in cylindrical coordinates by a vector potential with only a θ component:

$$A_\theta = \frac{B_0}{2} f(z) r, \tag{1}$$

where B_0 is the longitudinal (z coordinate) component of the magnetic field on the cathode and $f(0) = 1$. In (x, y) coordinates,

$$A_x = -\frac{B_0}{2} f(z) y; \quad A_y = \frac{B_0}{2} f(z) x. \tag{2}$$

If the kinematic momentum is zero at exit from the cathode, then the canonical momentum is $\vec{p} = -e\vec{A}$. The axial component of the canonical angular momentum of a particle at exit from the cathode is then

$$L_z = y P_x - x P_y \tag{3}$$

$$= \frac{eB_0}{2} r^2, \tag{4}$$

where e is the magnitude of the electron charge.

The 2-dimensional column vectors for the initial state in canonical coordinates, $X^c \equiv (x, p_x), Y^c \equiv (y, p_y)$, are related according to $Y^c = S_0^c X^c$, where

$$S_0^c \equiv \begin{pmatrix} 0 & -\frac{2}{eB_0} \\ \frac{eB_0}{2} & 0 \end{pmatrix} \tag{5}$$

and the superscript c indicates that we are in canonical coordinates.

Now propagate forward through the RF gun, the booster cavity, and other aspects of the system that are supposed to be cylindrically symmetric. The matrix M^c describing this propagation will be the same for both transverse degrees of freedom. At this point, $Y^c = M^c S_0^c (M^c)^{-1} X^c$, so the correlation matrix is $S^c = M^c S_0^c (M^c)^{-1}$. Given the skew diagonal form of S_0^c, it follows that $S_{2,2}^c = -S_{1,1}^c$.

At this point, canonical and kinematic momenta are equal, and the ambiguity in $x' \equiv p_x/p_z, y' \equiv p_y/p_z$ at the cathode no longer exists. The change in units from p_x to x' and p_y to y' does not change the relation between the diagonal elements of the correlation matrix. So the conclusion is:

$$S = \begin{pmatrix} a & b \\ -\frac{1+a^2}{b} & -a \end{pmatrix}, \tag{6}$$

where a and b are to be determined, likely by simulation.

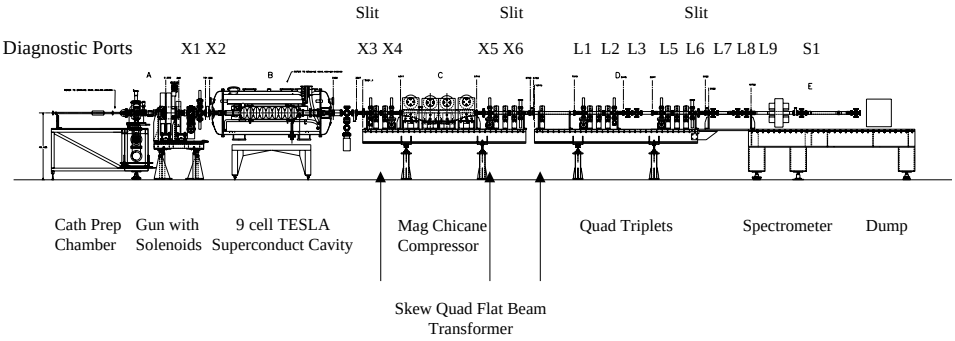

Figure 1: Layout of the FNPL photoinjector as related to this experiment.

3 THE SKEW-QUADRUPOLE CHANNEL

In our procedure the transformation was accomplished with three skew quadrupoles, as illustrated in Fig. 1 which depicts the layout of the Fermilab/NICADD Photoinjector Laboratory (FNPL).[1]

The 4×4 transport matrix through the skew quadrupole channel can be written in the form

$$M = R^{-1}TR, \tag{7}$$

where R is a coordinate rotation of 45^0 about the longitudinal axis:

$$R = \frac{1}{\sqrt{2}} \begin{pmatrix} I & I \\ -I & I \end{pmatrix} \tag{8}$$

and I is the 2×2 identity matrix. In the rotated coordinates, T represents a normal quadrupole channel, and so can be written

$$T = \begin{pmatrix} A & 0 \\ 0 & B \end{pmatrix}, \tag{9}$$

where A and B are 2×2 matrices. Using Eqs. 8 and 9. Eq. 7 becomes

$$M = \frac{1}{2} \begin{pmatrix} A+B & A-B \\ A-B & A+B \end{pmatrix}. \tag{10}$$

With $Y = SX$,

$$\begin{pmatrix} X \\ Y \end{pmatrix}_1 = \frac{1}{2} \begin{pmatrix} [A+B+(A-B)S]\,X \\ [A-B+(A+B)S]\,X \end{pmatrix}. \tag{11}$$

The condition for a flat beam in x is that Y_1 vanish. Since x_0 and y_0 are independent variables, this condition implies

$$A - B + (A+B)S = 0. \tag{12}$$

Let the three quadrupole strengths, $B'\ell/(B\rho)$, be q_1, q_2, q_3 separated by distances D_2 and D_3 in downstream progression.

In the thin lens approximation we find that the solution to Eq. 12 for q_1 is

$$q_1 = \pm\sqrt{\frac{-D_2 s_{1,1} + s_{1,2} - D_2 D_T s_{2,1} + D_T s_{2,2}}{D_2 D_T s_{1,2}}}, \tag{13}$$

[1]NICADD is the acronym for the Northern Illinois Center for Accelerator and Detector Development at Northern Illinois University.

with $D_T \equiv D_2 + D_3$, and the choice of sign is associated with the plane in which the beam is to be flat. For q_2 we have

$$q_2 = -\frac{s_{1,2} + D_T s_{2,2}}{D_2 D_3 (1 + q_1 s_{1,2})}. \tag{14}$$

The strength of the third quadruole, q_3, can be found from either term in the second row of Eq. 12. From the (2,1) element, we obtain

$$q_3 = \frac{-q_1 - q_2 - D_2 q_1 q_2 s_{1,1} - s_{2,1}}{1 + (D_T q_1 + D3 q_2) s_{1,1} + D_2 D_3 q_2 (q_1 + s_{2,1})}. \tag{15}$$

4 COMPARISON WITH SIMULATION

Throughout this experiment, we have relied on two codes, ASTRA [6] and HOMDYN [7] for simulation of propagation through the photoinjector. In this report, we base our comparison on ASTRA, and we anticipate that HOMDYN results will follow in the near future.

As in the past two years, we establish a waist in the beam at the OTR screen 0.2 m upstream of the first skew quadrupole (this drift distance is the missing D_1 from the equations of the preceding section). Then the solenoid settings and skew quadrupole gradients are adjusted to yield a flat beam at the exit from the skew quadrupole channel. We wish to compare the experimental results from measurements conducted in March 2002 with simulation.

The correlation matrix at entry to the skew quadrupole channel can be obtained by a least-squares fit to ASTRA prediction. A strong correlationwas found and is illustrated by Fig. 2 which shows a y' versus x plot just upstream of the skew quadrupole channel. Fig. 2 was produced with parameters associated with the running conditions. In contrast, if one turns space charge off in the simulation, the corresponding distribution is shown in Fig. 3. The fit to the simulation output yields for the correlation matrix at entry to the skew-channel

$$S = \begin{pmatrix} 0.713 \pm 0.071 & 3.556 \pm 0.211 \\ -0.405 \pm 0.026 & -0.719 \pm 0.076 \end{pmatrix}. \tag{16}$$

This fit was not constrained by the form for S in Eq. 6 and so it is gratifyingly close to the form suggested there.

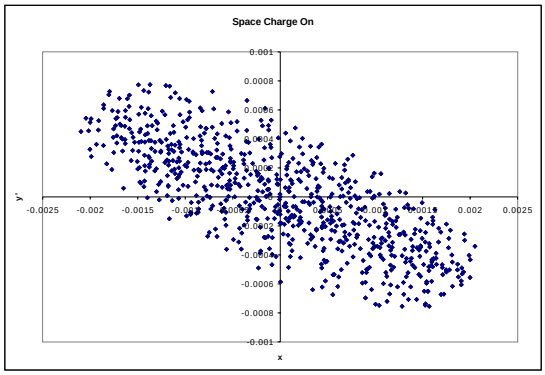

Figure 2: Simulation illustrating y', x correlation near entry to the skew-quadrupole channel Space charge is "on".

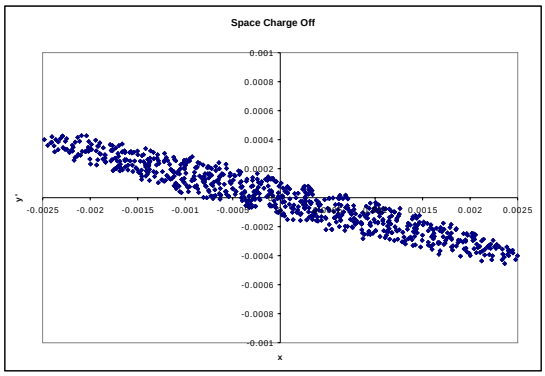

Figure 3: Simulation illustrating y', x correlation near entry to the skew quadrupole channel with space charge effects turned off.

At the end of the channel, one should find $S = \pm I$ where I is the identity matrix. The result of the ASTRA simulation gives

$$S = \begin{pmatrix} -0.998 & -0.003 \\ -0.029 & -0.930 \end{pmatrix}, \qquad (17)$$

and the change in $S_{2,1}$ through the last skew quadrupole is consistent with the strength of q_3.

The measurements indicated an emittance ratio of about 40 for a 10 ps 0.5 nC pulse; the ASTRA prediction was 46. (A space-charge-off run produced an emittance ratio of 290.) In Tab. 1 we list the comparison between predicted and observed values. Though the agreement between experiment and simulation is less than perfect, this is nevertheless the first occasion on which we feel that we are sufficiently close to report results in this context. The simulation results are very sensitive to the description of the laser spot on the cathode and the adjustment to minimum beam size on the OTR screen upstream of the skew quadrupole channel. Further investigation will be needed to quantify these sensitivities.

Table 1: Comparison between simulation and skew-quadrupole settings in recent measurements.

q-values m^{-1}	experiment	simulation
q_1	0.45	0.35
q_2	-0.62	-0.51
q_3	0.51	0.55

5 CONCLUDING REMARKS

Significant progress toward a high transverse emittance ratio electron beam has been made. In this third of our series of conference papers, we have presented improved understanding of the progress of angular momentum through the photoinjector. A paper covering this entire demonstration experiment is in preparation.

As we said in our first report, linear dynamics should work and it does. Much of the difficulty of pinning down the accuracy is of course instrumental. The observation of the variation with time of quantum efficiency and dark current depending on the magnetostatic surface fields on the cathode as investigated by Hartung[8] was a by-product of these measurements. Whether or not these are problems of a particular gun or cathode remains to be determined.

The fluctuations of bunch charge and profile from pulse-to-pulse and bunch-to-bunch at the photoinjector make results difficult to compare with the well-defined parameters of the simulations.

6 REFERENCES

[1] D. Edwards *et al*, "The Flat Beam Experiment at the FNAL Photoinjector", Proceedings LINAC2000.

[2] D. Edwards *et al*, "The Flat Beam Experiment at the Fermilab/NICADD Photoinjector Laboratory", Proceedings PAC2001.

[3] R. Brinkmann, Ya. Derbenev, and K. Flöttmann, "A Flat Beam Electron Source for Linear Colliders", TESLA Note 99-09, April 1999.

[4] Ya. Derbenev, "Adapting Optics for High Energy Electron Cooling", University of Michigan, UM-HE-98-04, Feb. 1998.

[5] A. Burov, Y. Derbenev, and S. Nagaitsev, "Circular Modes, Beam Adapters, and their Applications in Beam Optics", FERMILAB-PUB–01-060-T, May 2001, submitted to Phys. Rev. E.

[6] ASTRA was developed by K. Flöttmann. The manual and executables may be found at www.desy.de/ mpyflo.

[7] HOMDYN was developed by M. Ferrario. A description may be found in M. Ferrario *et al*, "HOMDYN Study for the LCLS Photoinjector", Proceedings Second ICFA Advanced Accelerator Workshop on the Physics of High Brightness Beams, Los Angeles, CA (1999).

[8] W. Hartung *et al*, "Studies of Photoemission and Field Emission from an RF Photo-Injector with a High Quantum Efficiency Photo-Cathode", Proceedings PAC 2001.